Manuscript for article in Robotica *(1996) vol. 4 pp. 321–327*

Design and Evaluation of a High-Performance Haptic Interface

R. E. Ellis O. M. Ismaeil M. G. Lipsett

Queen's University at Kingston, Ontario, Canada K7L 3N6

Abstract

For many dynamical tasks, a human performs better with force feedback or other haptic feedback than without; examples of such tasks are the teleoperation of a remote robot and the haptic interaction with a virtual environment. In order to accomplish these, or to conduct psychophysical experiments on haptics, it is desirable to have a computer-controlled mechanism that is able to detect relatively unimpeded motion and provide forces back to the human operator.

We have developed a prototype planar mechanism that satisfies many of the conflicting requirements on such a device. It has low apparent mass and damping, high structural stiffness, high force bandwidth, high force dynamic range, and an absence of mechanical singularities within its workspace. This paper presents a detailed analysis of the human-operator and mechanical constraints that apply to any hand controller, and proposed methods for the evaluation of haptic interfaces.

1 Introduction

One of the research efforts in our Robotics and Perception Laboratory is the construction of a device that can sense a human operator's hand motion, and actuate the operator with forces or torques without otherwise significantly impeding the hand motion. Such a device could be useful in such dynamical tasks as: the teleoperation of a remote robot; the characterization of human motor performance; the conduct of psychophysical experiments on haptics; and the interaction of a human a virtual environment. Application tasks that may benefit from dynamic teleoperation include the handling of materials in hazardous environments (such a nuclear or biological agents), the remote operation in an environment in which human presence is expensive to achieve and maintain (such as outside a space station or on the seafloor), and wherever human ability is physically limited (such as wielding large structures or performing microsurgery).

Common to all of these applications is the demand that the human operator or subject be as unimpeded as possible in motion, yet be provided with forces and torques that are of high fidelity. Although there is not yet a quantified determination of requirements for a given task, it is clear from the literature that many researchers seek to build a device with:

- Low apparent mass/inertia;
- Low friction;
- High structural stiffness;
- Backdriveability;
- Zero (or very low) backlash;
- High force bandwidth;
- High force dynamic range;
- Absence of mechanical singularities;
- Accessibility to the operator;
- Compactness; and
- An even "feel" through the workspace.

These demands are often conflicting, and difficult to achieve.

Our prototype planar mechanism meets all of these requirements except compactness. It is distinctive in using a parallel **X-Y** Cartesian positioning mechanism on which is mounted a rotary stage. Such a design is scalable both to larger displacements than are present in the prototype, and to a fully parallel spatial positioning mechanism, with little loss of performance.

After reviewing the state of the art in force-reflection (also called force-feedback) devices, we will describe how we arrived at our design, how we evaluated its performance, our assessment of the device aginst the evaluation criteria, and finally the contributions and implications of this work.

1.1 Previous Work

There has been considerable previous work in the areas of teleoperation, haptic feedback for virtual environments, and dynamic actuation of human limbs for identification or psychophysics. Common to all of these is that the purpose of the device is human actuation, and that the dynamics of the device are not directly coupled with the dynamics of the human except at a physically small interface. We specifically do not consider prosthetic devices and "power amplifying" devices here, because of two significant differences: a prosthetic device is in physical contact with the environment as well as with the human, so device dynamics are intimately and extensively coupled with the human; and a prosthetic device must be worn or carried, which produces design criteria that are very different from those of a more massive table-top force-feedback motion controller.

To date, most of the work on force-feedback controllers has been in the context of the *teleoperation* of remote robots. For the purposes of this paper, we define this activity to be the transmission of control variables from the human operator to the robotic device, in response to the transmission of feedback variables from the robot to the human.[1] It is common to denote the device which touches the human as

[1] A control variable is one which produces change in the mechanical state of the robot, and a feedback variable is one which produces a mechanical or psychological change in the human operator.

the *master*, and to denote the remote robot as the *slave*.[2] For an extensive survey, the reader is referred to a recent book by Sheridan [17]; articles that contribute to a perspective on the field have been written by Burdea and Zhuang [4, 5], and by Hannaford *et al.* [7].

Historically, teleoperation work was well under way by 1954, when Goertz and Thompson [6] described a manipulator developed at Argonne National Laboratories. Their ANL E-3 manipulator has six degrees of freedom, and can actuate a human with all 6 force/torque components. Capable of providing up to 8 pounds (about 35 N) in any direction, this device is severely limited by high static friction and a maximum guaranteed update rate of only 3 Hz. (Regrettably, these performance characteristics are typical of current commercial teleoperation master controllers, such as the Kraft Mini-Master.) The E-3 has been successfully used in virtual enviroments, particularly in the "docking" of large molecules [15, 16].

Higher performance was achieved in the 1970's, particularly at the Jet Propulsion Laboratory. Salisbury's Force-Reflecting Hand Controller [3] has six degrees of freedom, capable of actuating up to 9.8 N in force and 0.5 N-m in torque over a 30 cm^3 workspace. (The force bandwidth is not stated.) This device was later used by Hannaford *et al.* [7] to evaluate teleoperation task performance.

More recent devices have fewer degrees of freedom, with the explicit goal of larger mechanical bandwidth. A device with one degree of freedom has been used by Jones and Hunter [11] to study human perception of stiffness; the output bandwidth exceeded 1 KHz.

Several devices with two degrees of freedom have been developed. Mussa-Ivaldi *et al.* [14] examined the apparent stiffness in different arm postures, using a horizontal planar mechanism the performance of which is unstated. Howe and colleagues [8, 9] have used a vertical planar device, with a force bandwidth exceeding 100 Hz over a 5 N range, in telemanipulation experiments. Adelstein and Rosen [1] developed a spherical mechanism which can be controlled with high fidelity up to at least 48 Hz, at a sustained tip force of 20 N. (The performance of Howe's device and Adelstein's device may not be directly comparable, because of differences in testing methodology.)

A device with three degrees of freedom, developed by Hunter [10], uses three linear motors driving flexible beams in a closed kinematic chain. This arrangement produces extraordinary performance as a micromanipulator: for operation on the scale of an amphibian muscle cell, a bandwidth of 10 KHz is reported. A large master version has also been built, but regrettably the force bandwidth is unreported.

A device with four degrees of freedom is under development by Millman *et al.* [13, 12]. The design goal is 100 Hz with 10 pounds (44.5 N) force, but tested performance is not yet reported.

It is notable that all of the recent designs have attempted to place as many motors as possible on a single fixed base, and use closed-chain linkages to achieve output motion. Standard manipulators are of course built with the heavy motors as proximal as possible for performance reasons; for high-performance force control, we see a trend in the further use of closed-chain kinematics. This trend culminates in the six-degree-of-freedom Stewart platform, which is in common use in aircraft simulators and is clearly applicable to teleoperation devices.

[2] In human studies, the master is referred to as a *manipulandum*.

2 Design Issues and Constraints

Construction of force-feedback devices in our Laboratory is not directed towards a single application; we are interested in teleoperation, manipulation of virtual environments, and the psychophysics of human perception among other topics. In any such endeavour one must consider a wide variety of human and engineering constraints on the device design, such as those listed qualitatively in Section 1. These constraints warrant some discussion.

2.1 Human-Operator Constraints

The human requirements begin with the specification that the device be a hand controller, that is, that it have a "handle" grasped by the operator. To have this, one must also have the handle accessible to the human arm; for comfort, the human may be sitting. For mechanism simplicity, our prototype design was planar, and we chose the horizontal plane to be the plane of operation.

The minimum acceptable workspace for examining human arm motion is very large, and designing a device for full shoulder range is very challenging. To fully examine wrist motion, however, requires only the full radial-ulnar deviation and medial flexion-extension be achievable.[3] From our studies of human-wrist kinematics, we knew that a workspace of 15 cm × 15 cm easily contains the fingertip motion of normal adults, so this was chosen as the range of motion for the device.

Having determined the minimal positional range, the ranges of velocity and acceleration must be set. Again, our human-wrist studies indicate that the ideal device should be capable of moving at 2 m-s^{-1}, with a minimum peak acceleration of 8 m-s^{-2}. These high values have significant implications on the mechanism design as well as on the choice of actuator type, e.g., electrical and hydraulic actuators have better performance (respectively) in the velocity and force domains.

The human wrist is capable of exerting impressive force, especially if the forearm and body are appropriately braced. Normal adult males can easily exert over 200 N in medial flexion; since our concerns were not in simulating weightlifting but rather were directed towards more delicate manipulations, we chose a more modest 40 N force range.

The force bandwidth that the device must span is not trivial to determine. There are two principal considerations: at what frequency can the human wrist move, and at what frequency can the human hand perceive vibration. The former dominates motion studies (e.g. wrist pathology), and the second dominates psychophysics of touch and possibly teleoperation. Human wrist and finger tremor – especially the shiver reflex – easily exceeds 12 Hz, and can be 25 Hz for fingers. If the human is to be actuated at these frequencies, then the standard engineering practice indicates a force bandwidth of 40 Hz to 80 Hz, depending on the hand component that is to be studied.

[3] The human wrist can be closely approximated as having two degrees of freedom: a pair of non-orthogonal offset revolute joints.

The human fingertip is extraordinarily sensitive: single-point vibrations can be sensed to at least 300 Hz, and not uncommonly to 1000 Hz. These are over very small displacements, unlike large-displacement arm tremor; considering these to be different scales of operation, the designer must choose a scale over which the device operates or else face extreme demands on the device. For our prototype, we chose large-range and relatively small-bandwidth motion over short-range and high-bandwidth operation. Note that compared to ordinary robotic devices a force bandwidth of 100 Hz is still extraordinarily high, even for a planar mechanism.

2.2 Mechanical Constraints

Other design constraints arise from considerations of the mechanical interaction of the human with the device. Operator fatigue is a serious concern, especially for wrist motions that may be of a repetitive nature. This dictates that the apparent mass and inertia of any force-feedback device be kept low; casual study indicates that 50 g masses are acceptable for operations lasting 1/2 hour or less.

More problematic is friction: any mechanism whose motion involves contacting surfaces will have static friction. The only way to entirely eliminate this effect is to use non-contacting supports (e.g., air bearings or magnetic levitation). The minimum ineliminable friction force and the maximum force exertable by the mechanism/actuator system determine the force dynamic range; Adelstein and Rosen [1] chose a friction threshold that was 5% of the maximum exertable force as the design goal, based on the previous work of Bejczy and Salisbury [3]. This is a challenging requirement for a purely passive mechanical design.

The maximum stiffness that can be presented to a human operator who is in contact with the device's handle is no greater than the overall stiffness of the mechanism (including any linkages, transmissions, and sensors that are in series between the operator and the actuators. Unlike inertia and damping this cannot be compensated for in an control loop: it is an unavoidable constraint on the mechanical design. In particular, the structural elements of the mechanism must be stiff, as must all points of connection be. Attention must be paid to bearings and transmissions, as well as to the manner in which structural components are stressed.

Other mechanical constraints on a force-feedback motion controller derive from the constraint that the device provide high force fidelity. Aside from the obvious desire to correctly reflect the desired force in both direction and magnitude, any constant-force field must be presented in a homogeneous and isotropic manner. This is very difficult to achieve at low force values, where frictional effects (and in passive uncompensated devices, inertial effects) become dominant.

Finally, it is highly desirable that any force-feedback mechanism present no kinematic singularities in the operating workspace. A singularity entails the existence of an uncontrollable direction of motion, and consequently the existence of a direction in which force could not be applied to the operator.

2.3 Environmental Constraints

The anticipated environment in which the force-feedback device will be used may provide significant constraints on the design. As already noted, we expect our device to be operating in laboratories containing computers and robots, in psychophysical laboratories, and possibly in out-patient clinical settings. The three dominant actuator technologies are electrical, hydraulic, and pnuematic; using either of the latter two entails noisy or bulky power plants for system pressure. Hydraulics pose the possibility of leaking contaminating oils, and pneumatics are highly compliant actuators unless they are operated at high pressures. The previously stated constraints of rapid forceful motion tend to indicate hydraulics, but the anticipated operating environment tends to preclude them.

Hence, we decided upon electric actuation for our device. Because the maximum reasonable supply voltage and current in laboratory and clinical settings is a single-phase 120 VAC service, a maximum of 4 KW of power is assumed to be available for all power supplies, motors, fans, and associated electronics.

3 Design and Implementation

Serial mechanisms are compact and can be fast, but are not dynamically advantageous in the force domain. The major impediments to speed in serial mechanisms is the increase of total inertia and decrease in total stiffness, as measured in the base coordinate system, as each successively distal link is added to the chain. A particularly nettlesome tradeoff is actuator placement: actuation at the kinematic joint ("direct drive") eliminates or greatly reduces joint compliance, but the increase in inertia can be counteracted only by more proximal placement of actuators and the introduction of potentially compliant transmissions.

Parallel mechanisms do not always suffer from this defect. It is possible to produce a fully parallel mechanism with six degrees of freedom (the Stewart platform is an example). A significant advantage is the potential for placement of all actuators on a common baseplate, so that no actuator moves any other: each actuator moves only transmission elements or end-effector structures in addition to the payload. Parallel mechanisms also have a vast increase in structural stiffness compared to serial machanisms which is, regrettably, accompanied by either link intersection problems – mechanism elements physically interfere – or by the presence of kinematic singularities in all currently known designs. Fortunately, these conflicting design issues are mitigated somewhat by the constraints applicable to our particular device.

Our prototype device is intended for planar operation, so there are only three degrees of freedom to be achieved. Simple combinatorics, with the observation that a single parallel linkage is equavalent to a single serial linkage, indicate that these can be acheived with combinations of serial and parallel mechanisms in only a few ways:

- 3 serial; or
- 1 serial and then 2 parallel; or
- 2 parallel and then 1 serial; or
- 3 parallel.

The latter choice is a Stewart-like arrangement [12], but suffers from internal singularities over a full 2π range of orien-

tation. Taking maximum advantage of the inertial/stiffness advantages of parallel actuation leads inevitably to consideration of a 2-parallel, 1-serial planar mechanism.

Rather than using the 5-bar linkage [8] for parallel actuation, we have chosen a parallel Cartesian planar mechanism. This design choice decoupled the kinematics and dynamics of the axes, and allowed the motors to be mounted on a stable shared baseplate. We expected that the use of light frames, and precision linear anti-friction bearings, would give the mechanism excellent structural strength without excessive mass. Such an arrangement would either have to use a transmission element to convert servomotor rotation to translation, or use a linear motor; cost, force considerations, and ease of control indicated use of a DC servomotor and a transmission.

3.1 Mechanical Design

Our parallel Cartesian mechanism is a departure from the traditional serial **X**/**Y** stage, in which the **X** motor must actuate both the environmental load and the **Y** motor/linkage. Using two independent linear stages, each with a projecting rod that passes through a common block that moves, produces a linkage that is mechanically parallel and kinematically orthogonal. An illustration of the **X**-**Y** conceptual design is given in Figure 1; in implementation, the two opposing side blocks for each axis must be tied by a space-frame structure to eliminate undesired flexure. A low-mass rotary joint, mounted on the handle block, completes the planar mechanism; a side view of the moving handle components is given in Figure 2.

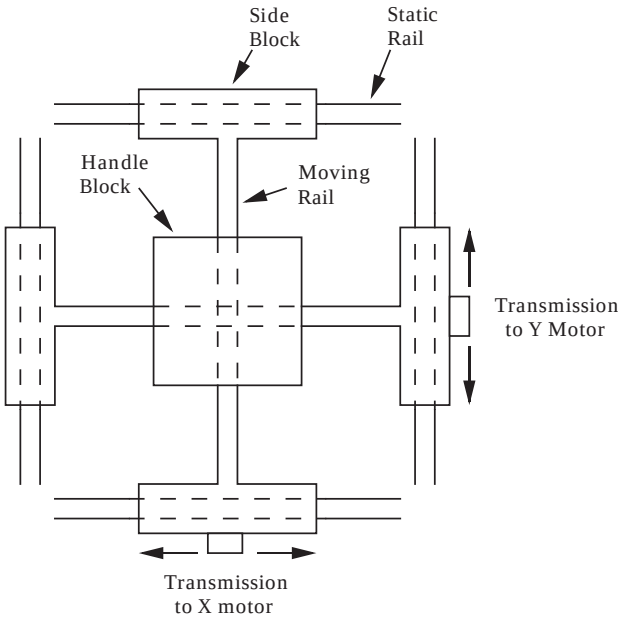

Figure 1: A schematic of the **X**-**Y** mechanism. Motion of a sideblock moves its opposite block and the handle block.

To produce the linear motion of each axis, we installed precision linear bearings; from the known maximum force the device would provide, and standard engineering references, we determined that 6.25 mm were the smallest that

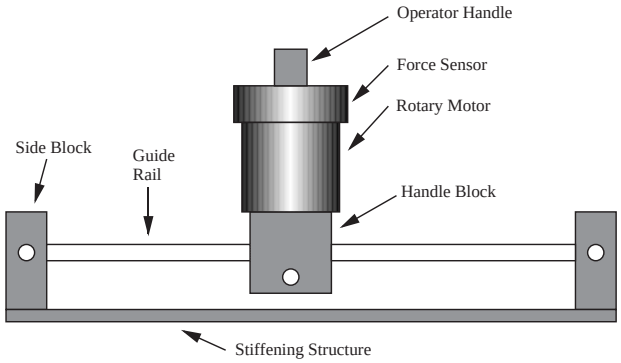

Figure 2: Vertical assembly of the mechanism **X** axis. This assembly moves along rails through the side blocks; the handle block moves with it, and also is moved laterally by an orthogonal **Y** assembly that is of similar construction.

could reliably carry the maximum load. These bearings are light, have low backlash, extremely low frictional coefficients (static coefficient of 0.0024, rolling coefficient of 0.0012), and excellent wear characteristics. They were fit to AISI-1060 shafts hardened to a nominal Rockwell 60C, with two bearings per shaft. Standard silicone lubricants are applied to the exposed rods weekly, or before any significant test.

The play in the bearings produced a troublesome effect in the original test version. Referring to Figure 1, we see that if the side block is held fixed by the motor and the opposite block is forced, then the intervening shaft can deviate from its original orthogonal alignment. (Part of this is due to shaft deflection, which is easily addressed by additional stiffening members.)

The two alternatives considered were to pre-load the bearings, or to introduce additional members into the linkage. The bearing pre-load option increased the frictional behavior to a palpably unacceptable level, and was rejected. Thus, we produced a small moving frame for each axis that dramatically reduced the alignment errors at the cost of a less compact device. The calculations for alignment play are just simple trigonometry dependent on the values of the angular play and the sideplay in each bearing. These procedures are scalable in the sense that if a larger workspace is required, the calculations are valid until deformation of the structure must be taken into account.

The moving structures are aluminum for lightness, and the linear-bearing rods must be steel for hardness. This introduces a possibility of thermal-expansion effects. We mounted the rods, via aluminum posts, to a thick steel plate for rigidity and to match the thermal expansion of the steel rods. Normal laboratory temperature ranges (15° C to 25° C) produce no discernible temperature effects. A photograph of the assembled mechanism is presented in Figure 3.

One troublesome mechanical component is the rotary-to-linear transmission that connects the DC servomotor to the mechanism. Standard solutions, such as ball screws or rack-and-pinion drives, are inappropriate. The former have high inertia that limits the output force bandwidth, are not adequately backdriveable without prohibitively expensive special-pitch machining, and have backlash that cannot be eliminated without friction-inducing preload; the latter have

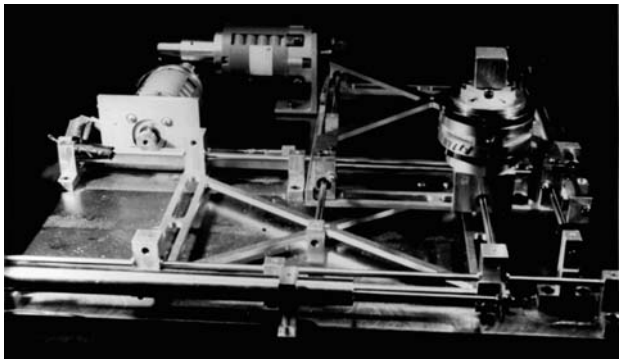

Figure 3: Photograph of the planar haptic interface.

either backlash or interference (depending on the preload), and also have nonlinearities due to microscopic tooth differences and macroscopic alignment difficulties.

Hence, we chose cable drives. These have low inertia, low friction, high bandwidth, and are eminently backdriveable. Our pulleys are motor-mounted free-machining brass, and currently our cables are Teflon-coated stainless steel. The cables are tied at each end of an axis side-block, one end fixed and the other end adjustable to vary the cable tension; the arrangement is depicted in Figure 4.

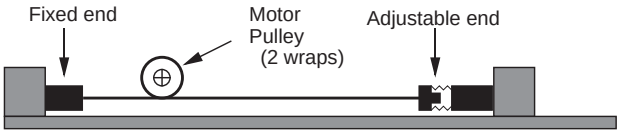

Figure 4: Drive cabling for a linear axis.

3.2 Actuation and Sensing

The selection of rotary DC servomotors and cable transmission, plus the desire for homogenous force transmission, dictated much of the associated sensors and electronics. We used low-inertia brushed DC motors, powered by linear current amplifiers. Although less compact than pulse-width-modulation amplifiers, and demanding more heat dissipation, linear amplifiers provide a faithful transformation from input voltage to motor torque without the "scratchy" feeling and high-frequency auditory noise associated with PWM amplifiers.[4] To ensure that no amplifier electronic cross-talk could occur, each is independently transformer-isolated from the AC main.

High-performance sensing is needed for motion that occurs at 100 Hz or more.[5] To sense motor position and thus be able to compensate for motor nonlinearities, we chose resolvers and digital converters with a nominal resolution of 3.5 arc-minutes (0.006 rad) and an acceleration constant of up to 35,500 s^{-2}. Although very accurate, the conversion is limited to speeds of 8 rotations per second, so the resolvers cannot be used to deduce high-speed motion. They are, however, excellent for detecting low-speed motion where frictional effects dominate.

[4] Even with a switching frequency above 20 KHz, a PWM can excite audible and palpable subharmonics in a mechanical structure.

[5] Our force-feedback control law includes position-dependent components.

The motion of the mechanical structure may differ from that of the motors, because of transmission compliance. To ensure that the actual handle motion is known accurately, and to detect high-speed motion accurately, we installed 400 Hz LVDT's on the side blocks. Using 12-bit analog-to-digital conversion, linear motion of 0.03 mm is easily detectable. Combining the resolver and LVDT outputs in a three-point forward-difference scheme gives observed velocity over a wide range.

The final sensing component is a force/torque sensor mounted between the distal axis and the 25 mm cube that acts as the operator handle. The Assurance Technologies FTS 15/50 is a 6-axis sensor with integral signal conditioning and 12-bit analog-to-digital conversion; it detects up to ±66 N of force in increments of 0.14 N at 400 Hz. This sensor is used to determine the differential force between the mechanism and the human operator, so that a feedback loop can be used to compensate for unmodelled components of the device dynamics.

3.3 Computer Control

In order to provide ease of development, compatibility with existing hardware and software, and modularity, we have separated the real-time device controller from the computer responsible for computing virtual environments and/or interfacing to robot arms. A SPARC-2 engineering workstation from SUN Microsystems acts as the host on which software is developed; control code is then downloaded, via a Performance Technologies bus adaptor, to a VME board that contains a pair of Texas Instruments TMS320C30 digital-signal-processing computers (from SKY Computers Inc.). The board contains two 34 MFLOP processors, and 2 MB of memory that is sharable with the host. Analog data from the LVDT sensors are acquired with Analog Devices 12-bit A/D VME cards; analog signals to the amplifiers are produced by independent Analog Devices 12-bit D/A VME cards; and a custom VME card acquires resolver and force/torque data.

After determining data and bus-control dependencies, we decided upon a static task allocation between the two processors. One processor acquires the force/torque data from the operator handle, and in teleoperation mode also reads forces and torques from a 1000 Hz 6-axis wrist sensor made by Zebra Robotics. These data are placed in global memory. On the other processor resolver data are acquired and,

using force/torque data and desired-force data from either the host or the slave robot, a control loop determines the amplifier output current to the motors. The D/A converters are updated at 1200 Hz; this rate includes all data acquisition, timing coherence, and control computations. The computational architecture is indicated in Figure 5.

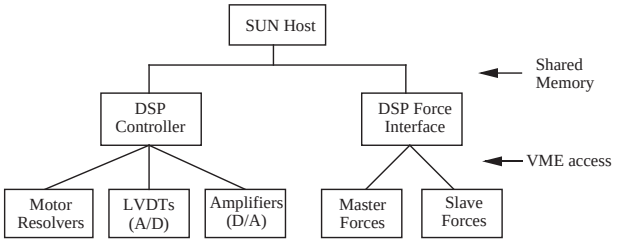

Figure 5: Computational architecture.

Kinematic orthogonality among the mechanism axes implies dynamic decoupling of the axes, so three independent controllers can be used. The forward dynamics of each axis is very simple – the stiffness of the transmission and linkage components is so high that a single lumped-parameter model seems to suffice. The inertia of the motor, transmission, and linkage is combined for each axis, as are the motor viscous friction and the linear-bearing viscous friction. These form a standard second-order linear system, from which two controllers can be developed. Treating the device as a force-feedback manipulandum we use a force controller, and treating the device as a conventional robot we use a PI position controller. Unmodelled dynamical effects seem to be adequately managed by the high servo rate of the DSP-based control loop. A block diagram of the overall system, in force-control mode, is shown in Figure 6.

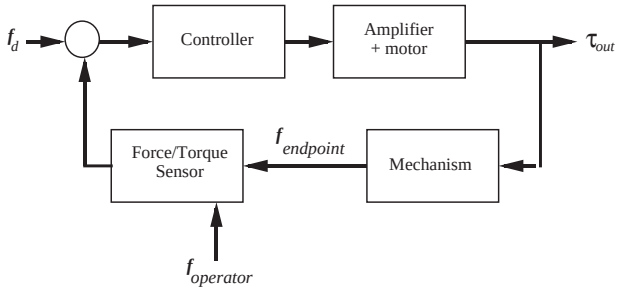

Figure 6: Overall system block diagram

The greatest impediment to high force performance by our mechanism is friction, especially static friction. We attempted to alleviate the friction by carefully mapping the static friction, as suggested by Armstrong-Hélouvry [2]. Position-dependent feed-forward control is then used to compensate for the variable friction, which include both motor and linkage effects. The force-control block diagram is given in Figure 7.

4 Device Evaluation

We have evaluated the performance of our planar haptic interface by examining it in three ways. Considered as an open-loop mechanism, we examined the structural dynamics to determine the fundamental frequency-response characteristics of the actuated linkage. Considered as a force-controlled robot, we examined the force characteristics, and

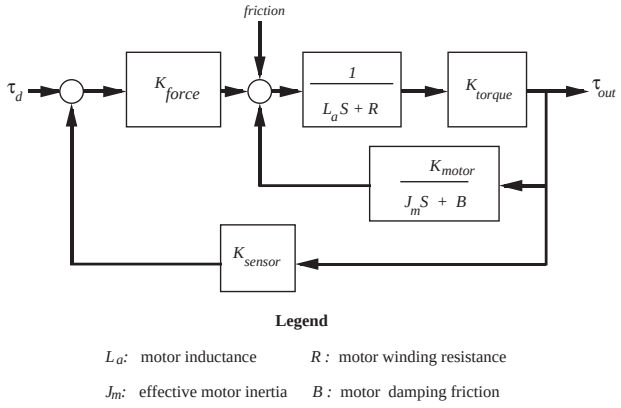

Figure 7: Force-control block diagram

considered as a position-controlled robot we examined the traditional positioning and overall stiffness. This lead to evaluations of

- Structural dynamics;
- Force range and bandwidth;
- Positional range, accuracy, and repeatability; and
- PI controller stiffness.

For each of these, we were interested in not only performance but also in appropriate methodology – in a repeatable and reproducible way to determine relevant characteristics.

All of the tests we present were conducted on the **X-Y** force mechanism, with the rotary stage removed;[6] in place of the latter we used an aluminum block of the appropriate mass. Thus, although we evaluate only the positioning mechanism we believe that the results appropriately measure the overall device performance.

4.1 Structural Dynamics

We examined the structural dynamics by estimating the frequency response function nonparametrically. Our specific interest was in the gain of accelerations across the low-frequency spectrum, as a function of the input commands to the motor amplifiers. The system tested is depicted in Figure 8.

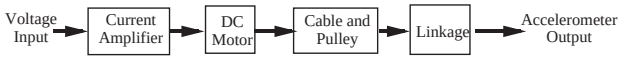

Figure 8: System tested for structural dynamics.

Methodology A Hewlett-Packard pseudo-random noise generator (model 3722A) supplied the input to a single mechanism axis. A Brüel & Kjær piezoelectric accelerometer (model 4393) was applied to the operator handle with beeswax; a Brüel & Kjær charge amplifier (model 2635) converted the accelerometer output to a voltage. The input signal and the output signal were fed to a WAVEPAK data acquisition and analysis system (from Computational Systems Incorporated) that was installed on an IBM-compatible microcomputer. WAVEPAK digitization was performed with dual high-speed 12-bit converters.

[6] At the time of writing, the rotary motor is undergoing redesign.

The dynamics were examined on the translational axes independently in 9 distinct **X-Y** positions. The noise generator was set to the maximum amplitude that did not result in the mechanism contacting the limit stops, and the charge amplifier was set to ensure no signal overload and consequent clipping. Structural coupling was tested by applying the input to one translational axis and examining the response of the other translational axis.

The data were analysed with WAVEPAK by performing a fast Fourier transform, and plotting the transfer function (gain) according to frequency. The results of 16 individual scans were averaged; this number was selected because introducing more scans did not further sharpen the response curves.

Results The test results in each individual configuration were highly repeatable. A sample transfer function and a lumped-parameter approximation are shown in Figure 9; the experimental phase is shown in Figure 10. (Note that the motor offsets the phase by 90°.) The 90 Hz gain peak corresponds with the phase roll-over point, indicating a structural resonance; the parametric model also exhibits this behaviour, albeit differently.

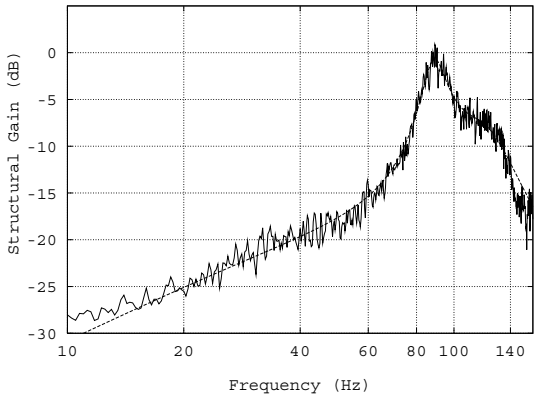

Figure 9: Typical structural-dynamics response curve.

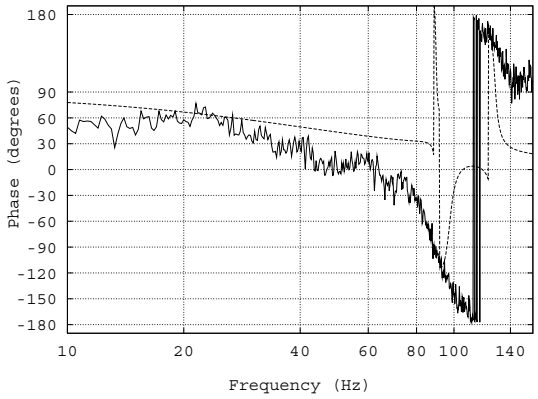

Figure 10: Typical structural-dynamics phase plot.

To ensure that we were not observing motor/amplifier effects, we independently tested the motors by placing a short, stiff aluminum lever bar on the shaft. This bar, with an inertia calculated to be that of the actual movable mechanism, had an accelerometer affixed to the end. We observed excellent gain and phase correlation up to 90 Hz, beyond which was a profound resonance most likely due to motor-shaft windup. To ensure that the cable transmission was not a problem, we placed an accelerometer immediately adjacent to the fixed end of the cable; the first resonance occurred at approximately 300 Hz. We do not believe that the motors or cable transmissions are significant limitations.

4.2 Force Control

There are at least four force measurements that are of interest in evaluating the performance of a haptic interface:

1. Maximum applicable force;
2. Static-friction force;
3. Minimum controllable force; and
4. Force bandwidth.

The first two can be measured with an open-loop command, and the third can be measured by voluntary human motion during closed-loop control, but the fourth requires closed-loop control against an object of known and unchanging impedance. To determine the bandwidth, we measured the device response against a readily obtainable polymer that has mechanical characteristics comparable to moderately tonic muscle. (Muscle stiffness varies by a factor of at least 10 for any given normal individual, so a reference material is needed.)

Force-Magnitude Methodology The steel baseplate of the mechanism was clamped to a heavy table, as was a stiff aluminum jig. The proportional force controller modelled only the estimated mechanism inertia and motor torque constant. We adhered to a flat face of the jig an approximately hemispherical molding of Sorbothane shock-absorbing polymer, 50 mm in diameter and 24 mm in height (obtained from Edmund Scientific Company as a shock mount for optical equipment). The handle contact, when needed, was between two Sorbothane blocks that were clamped to simulate a moderate grasping force.

The maximum force was measured by having the computer command a constant value to the actuators; the endpoint force sensor reported the resulting force. The minimum force, which represented the static-friction breakaway force, was measured by placing the device far from contact with the jig. Open-loop values were maintained for three seconds, and the value was deemed to be a breakaway value if motion occurred that exceeded 2 least-significant bits of the LVDT position sensor. (This was done for the entire workspace, in accordance with the procedure recommended in [2].) From the known relation between output values and endpoint force, we calculated the breakaway force.

The minimum controllable force was measured by commanding a closed-loop proportional controller to maintain a zero differential force on the operator handle; the minimum force that induced motion, and the peak force during motion, give estimates of the sensitivity of the device. Our procedure was to move the device by voluntary hand motion, and record the position and handle force. We noted

the least force required to initiate or maintain motion, and the maximum force during the trial.

Force-Bandwidth Methodology The handle was grasped by the Sorbothane jig, as described above. The computer commanded the device to maintain an offset-sinusoidal differential force; the peak amplitude was 50% of the maximum obtainable DC amplitude, and the minimum amplitude was 12.5% of the maximum DC amplitude. This is similar to Howe's method [8]. The sinusoid was computed in the same processor as the controller, and we scanned the frequencies between 10 Hz and 140 Hz. The scan was performed 3 times, and the peak-to-peak force amplitudes were averaged at each frequency.

Results With the current reduction ratios of the pulley/cable transmission, we observed a maximum open-loop force of 56 N and a minimum open-loop breakaway force of 1.7 N. This indicates a static-friction level that is 3% of the maximum force output, which is well within the 5% guidelines described in Section 2.2. The minimum closed-loop force inducing motion is 0.42 N, about 1/4 of the static friction; the maximum closed-loop force during vigorous voluntary manipulation is 8.3 N.

The force-controlled response is not unusual. The response is strong below 20 Hz, and around 40 Hz, with a corner at 70 Hz. The current implementation has usable gain up to at least 80 Hz.

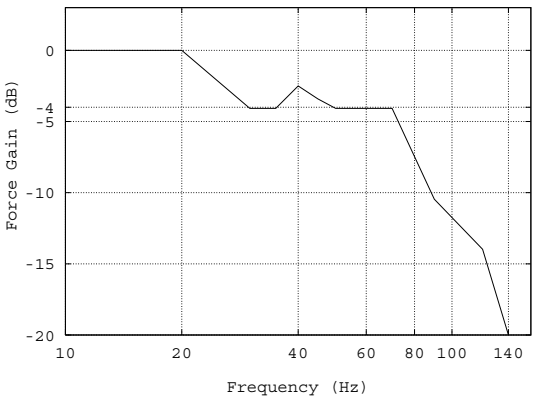

Figure 11: Frequency-gain plot of the force controller.

We are not currently certain of the sources of the peaks, but structural resonance and self-damping are suspected. Flattening the frequency-response curve is an obvious future direction for our work.

4.3 Position Control

A conventional evaluation of robotic devices is the accuracy and repeatability of positioning behaviour. For completeness, we include assessments of our force-feedback motion controller as a conventional robot. Of particular interest is the maximum DC stiffness, which indicates total device flexure under the largest proportional gain that can be used without inducing control instabilities.

Methodology For positioning tests, machined blocks of known dimensions, and mechanism limit stops, were used to produce fiducial reference positions within the workspace. The device was moved by hand (power off) to these reference positions, and LVDT readings taken to establish the device coordinates of the positions. The device was then deviated from the reference positions, and when handle motion ceased the positioning was examined using the machined blocks. Multiple readings determined the accuracy and repeatability.

For stiffness tests, the computer was set to implement a simple proportional (P) controller, so that integral (I) compensation did not cause saturation. The handle was deviated from a fiducial reference position by a linear micrometer stage (calibrated in 1/100 millimeter increments); the micrometer maintained unilateral contact throughout. For a given deviation, the applied force was read from the force/torque sensor in the handle assembly; the resulting position and force relation gave a DC stiffness. A human gripping the handle was unable to induce instability (although releasing the grip and striking the handle hard with a knuckle produced oscillation).

Results Unlike most robots, our planar haptic interface has independent parallel actuation of orthogonal axes, and additionally has sensors that detect the motion nearly at the endpoint (rather than at a remote joint). Typical robots have good repeatability, but much poorer accuracy.

The positioning tests indicate that the repeatability and accuracy are the same: plus or minus 1 least-significant bit of the LVDT sensors, or ± 0.03 mm in either Cartesian axis. This implies the ability to determine very accurately the net hand motion of a human operator.

The stiffness tests indicate a DC stiffness of $24,000\ \mathrm{N{\cdot}m^{-1}}$ when the controller is set to its maximum stable gain. This measurement includes all sources of passive compliance in the mechanism. At this stiffness a human cannot easily induce control instabilities by voluntary motion, but can do so by holding the handle and simultaneously striking the handle with a rigid object.

4.4 Assessment

Overall, we believe that we have designed and constructed a force-feedback motion controller that is appropriate for use in human motor and perceptual studies. The operating characteristics are summarized in Table 1.

Two characteristics require further work: the compactness of the device, and a slightly peculiar "feel" that is due to the so-called quadrature error induced by residual static friction. The layout of this prototype could be improved; a greater ratio of motion workspace to overall footprint is desirable. More problematic is that this device, like any Cartesian mechanism, has dynamics that are homogeneous but anisotropic; a diagonal motion is the sum of orthogonal motions, and at the outer operating limits of the device (maximum and mimimum forces) the inability of the compensator to remove all device native dynamics are apparent. Improving the dynamical model and increasing the dynamic range of the force sensor may help to reduce these effects.

Table 1: Device Characteristics

Base dimensions	65 cm × 65 cm
Workspace	15 cm × 15 cm
Positioning repeatability	0.03 mm
Positioning accuracy	0.03 mm
Peak velocity	$1.2\ \mathrm{m \cdot s^{-1}}$
Peak acceleration	$30\ \mathrm{m \cdot s^{-2}}$ (3 g)
Maximum exertable force	56 N
Passive static-friction force	1.7 N
Minimum force felt	0.4 N
Maximum force felt	8.3 N
First structural resonance	90 Hz
Force bandwidth	80 Hz
Maximum stiffness	$24,000\mathrm{N \cdot m}$

5 Conclusions

We have conducted an analysis of the important design considerations which must be addressed in the development of a hand controller, and produced a planar haptic interface that satisfies those considerations. We have also developed a detailed, reproducible methodology for the evaluation of hand-controller operating characteristics.

Our device is a fast, powerful, sensitive mechanism useful for studying force feedback in a variety of domains. It features an unusual Cartesian linkage that decouples the kinematics, considerably simplifying the dynamical behaviour. The controller is a powerful digital-signal-processing system that produces high update rates despite the complexity of the friction compensators. The mechanism can be enlarged without much degradation in performance.

The prototype mechanism is planar, but we are currently extending the design to provide a fully parallel spatial mechanism with similar operating characteristics. Of the many potential uses for our prototype, one that is particularly intriguing is examination of how a human operator perceives force – a crucial design concern in the development of the next generation of force-feedback hand controllers.

Acknowledgements

This research was supported in part by the Natural Sciences and Engineering Research Council of Canada and the federal government under the Institute for Robotics and Intelligent Systems (which is a National Centres of Excellence programme). We gratefully acknowledge the assistance of Dr. Vincent Hayward of McGill University, for suggesting the use of DSP's for control.

References

[1] B. D. Adelstein and M. J. Rosen. "Design and implementation of a force reflecting manipulandum for manual control research". In *Advances in Robotics: 1992, DSC Volume 42*, pages 1–12. American Society of Mechanical Engineers, 1992.

[2] B. Armstrong-Hélouvry. *Control of Machines with Friction*. Kluwer Academic Publishers, Boston, 1991.

[3] A. K. Bejczy and J. K. Salisbury Jr. "Controlling remote manipulators through kinesthetic coupling". *Computers in Mechanical Engineering*, 2(1):48–60, 1983.

[4] G. Burdea and J. Zhuang. "Dextrous telerobotics with force feedback – an overview. Part 1: Human factors". *Robotica*, 9:171–178, 1991.

[5] G. Burdea and J. Zhuang. "Dextrous telerobotics with force feedback – an overview. Part 2: Control and implementation". *Robotica*, 9:291–298, 1991.

[6] R. C. Goertz and R. C. Thompson. "Electronically controlled manipulator". *Nucleonics*, pages 46–47, 1954.

[7] B. Hannaford, L. Wood, D. A. McAffee, and H. Zak. "Performance evaluation of a six-axis generalized force-reflecting teleoperator". *IEEE Transactions on Systems, Man, and Cybernetics*, 21(3):620–633, 1991.

[8] R. D. Howe and D. Kontarinis. "Task performance with a dextrous teleoperated hand system". In *Proceedings of the SPIE Conference on Telemanipulator Technology (OE/Technology '92), in press*, 1992.

[9] R. D. Howe. "A force-reflecting teleoperated hand system for the study of tactile sensing in precision manipulation". In *Proceedings of the IEEE International Conference on Robotics and Automation*, pages 1321–1326, 1992.

[10] I. W. Hunter, S. Lafontaine, P. M. F. Nielsen, P. J. Hunter, and J. M. Hollerbach. "Manipulation and dynamic mechanical testing of microscopicobjects using a tele-micro-robot system". In *Proceedings of the IEEE International Conference on Robotics and Automation*, pages 1553–1558, 1989.

[11] L. A. Jones and I. W. Hunter. "Influence of the mechanical properties of a manipulandum on human operator dynamics: I. elastic stiffness". *Biological Cybernetics*, 62:299–307, 1990.

[12] P. Millman and J. E. Colgate. "Design of a four degree-of-freedom force-reflecting manipulandum with a specified force/torque workspace". In *Proceedings of the IEEE International Conference on Robotics and Automation*, pages 1488–1493, 1991.

[13] P. Millman, M. Stanley, P. Grafing, and J. E. Colgate. "A system for the implementation and kinesthetic display of virtual environments". In *Proceedings of the SPIE Conference on Telemanipulator Technology (OE/Technology '92), in press*, 1992.

[14] F. A. Mussa-Ivaldi, N. Hogan, and E. Bizzi. "Neural, mechanical, and geometric factors subserving arm posture in humans". *The Journal of Neuroscience*, 5(10):2732–2743, 1985.

[15] M. Ouh-young, M. Pique, J. Hughes, N. Srinivasan, and F. P. Brooks, Jr. "Using a manipulator for force display in molecular docking". In *Proceedings of the IEEE International Conference on Robotics and Automation*, pages 1824–1829, 1988.

[16] M. Ouh-young, D. V. Beard, and F. P. Brooks, Jr. "Force display performs better than visual display in a simple 6-d docking task". In *Proceedings of the IEEE International Conference on Robotics and Automation*, pages 1462–1466, 1989.

[17] T. B. Sheridan. *Telerobotics, Automation, and Human Supervisory Control*. MIT Press, Cambridge MA, 1992.